

## Mechanism of single-bubble sonoluminescence

Kyuichi Yasui

*National Industrial Research Institute of Nagoya, 1-1 Hirate-cho, Kita-ku, Nagoya 462-8510, Japan*

(Received 7 July 1998; revised manuscript received 3 May 1999)

The mechanism of the light emission of single-bubble sonoluminescence (SBSL) is studied theoretically based on the quasiadiabatic compression model. It is concluded that SBSL is not the blackbody radiation but the thermal radiation. It is clarified that the shape of the spectrum is determined by the temperature inside the bubble and the intensity is determined by the rates of the microscopic processes of the light emission. For a noble-gas bubble, radiative recombination of electrons and ions and electron-atom bremsstrahlung are the dominant microscopic processes of the light emission, and the intensity is mainly determined by the degree of ionization of the gas inside the bubble. It is also clarified that for a noble-gas bubble the pulse width of the light is nearly independent of wavelength. [S1063-651X(99)10708-6]

PACS number(s): 78.60.Mq

### I. INTRODUCTION

Single-bubble sonoluminescence (SBSL) is a light emission phenomenon from a stably oscillating bubble in liquid irradiated by the ultrasonic wave [1]. SBSL was first reported by Gaitan *et al.* [2] less than ten years ago. Since the discovery, many researchers have investigated SBSL both experimentally and theoretically [3]. However, the mechanism of the light emission of SBSL is still unclear [3].

There are two theoretical models of the bubble collapse under a condition of SBSL. One is the shock-wave model [4–6] in which a spherically symmetric shock wave develops inside the bubble and converges at the center of the bubble. The light is emitted from the bubble center where plasma is created by the shock-wave convergence. The other is the quasiadiabatic compression model [7,8] in which no shock wave develops inside the bubble and the whole bubble is heated up by the quasiadiabatic compression (“quasi” means that appreciable thermal conduction takes place between the bubble and the surrounding liquid).

Recently, Weninger *et al.* [9] observed sonoluminescence from an isolated bubble on a solid surface (a hemispherical bubble) and found that the spectrum is similar to that of SBSL. It suggests that the mechanism of sonoluminescence from the surface bubble is the same as that of SBSL. This disagrees with the shock-wave model because the surface bubble is not an accurate hemisphere due to the frictional force at the solid surface. For the shock-wave convergence, it should be an accurate hemisphere.

Theoretically, Vuong, Szeri, and Young [10,11] clarified that no shock wave develops inside a noble-gas bubble by numerical simulations of the gas dynamics within a collapsing bubble, taking into account the diffusive transport such as thermal conduction and viscosity. It should be noted that the diffusive transport inside a bubble has been neglected in the numerical simulations of the shock-wave model [4–6]. The reason for the no shock formation is described in detail in Ref. [11]. Recently, Yuan *et al.* [12,13] also showed that no shock wave develops inside a SBSL bubble by numerical simulations of the gas dynamics including the diffusive transport. Thus, it is expected that no shock wave develops inside a SBSL bubble and the whole bubble is heated up

almost uniformly. In the present study of the mechanism of the light emission, the quasiadiabatic compression model [8] is used.

In the first part of the present paper, a result of the computer simulation of radiation processes inside an argon bubble under a condition of SBSL is presented. In the latter part of the paper, the theoretical analysis of the experimentally observed spectra of SBSL [14,15] is presented.

### II. MODEL

In the present study, a computer simulation of radiation processes inside an argon bubble is performed under a condition of SBSL. The model of the bubble dynamics is fully described in Ref. [8]. In the model [8], the pressure is assumed to be spatially uniform inside a bubble and the temperature is assumed to be spatially uniform inside a bubble except at the thermal boundary layer near the bubble wall whose thickness is  $n\lambda$ , where  $n$  is a constant and  $\lambda$  is the mean-free path of a molecule (in the present calculation,  $n = 7$  is assumed [16]). In the present model [8], the effect of thermal conduction both inside and outside a bubble, that of nonequilibrium evaporation and condensation of water vapor at the bubble wall, and that of chemical reactions inside a bubble are taken into account.

The following is the present model of radiation processes inside a bubble. The number of free electrons ( $n_e$ ) inside a bubble is calculated by the Saha equation [4,17].

$$\frac{q^2}{(1-q)} = 2.4 \times 10^{21} T^{3/2} e^{-\chi/kT} \frac{1}{N}, \quad (1)$$

$$n_e = \frac{4}{3} \pi R^3 q N, \quad (2)$$

where all the quantities are expressed in Système International (SI) units,  $q$  is the degree of ionization,  $T$  is the temperature,  $\chi$  is the ionization potential of the gas,  $k$  is the Boltzmann constant,  $N$  is the number density of atoms, and  $R$  is the bubble radius. The ionization potential of argon is  $\chi = 15.8 \text{ eV} = 2.53 \times 10^{-18} \text{ J}$ .

The spectra of SBSL are continuous and have no characteristic lines such as the OH line [14,15]. In the temperature range considered here (10 000–20 000 K), the continuous spectra from noble gases are due to radiative recombination of electrons and ions or thermal bremsstrahlung of electrons [17]. Radiative attachment of electrons to neutral atoms is neglected because noble gases do not form stable negative ions [18]. The rate of radiative recombination ( $r_r$ ) is estimated by

$$r_r = \frac{4}{3} \pi R^3 q^2 N^2 \sigma_{fb} \bar{v}, \quad (3)$$

where  $\sigma_{fb}$  is the cross section of radiative recombination and  $\bar{v}$  is the mean velocity of a free electron ( $\bar{v} = \sqrt{8kT/\pi m_e}$ , where  $m_e$  is the electron mass). The cross section of radiative recombination of hydrogen is known to be on the order of  $10^{-25} \sim 10^{-23}$  (m<sup>2</sup>) [19] depending on the initial electron velocity and the final energy state. The cross section of argon is not known but it is probably on the same order as that of hydrogen or even larger [19]. Thus in the present calculation,  $\sigma_{fb} = 10^{-24}$  (m<sup>2</sup>) is assumed.

For the thermal bremsstrahlung, two mechanisms exist: electron-ion bremsstrahlung [17] and electron-atom bremsstrahlung [20,21]. The electron-ion bremsstrahlung is the light emission from an electron accelerated in the Coulomb field of a positive ion, and the intensity is given by [4,17]

$$P_{Br,ion} = 1.57 \times 10^{-40} q^2 N^2 T^{1/2} \pi R^3, \quad (4)$$

where all the quantities are expressed in SI units. The electron-atom bremsstrahlung is the light emission from an electron accelerated in the field of a neutral atom, and the intensity is crudely estimated by [21]

$$P_{Br,atom} = 4.6 \times 10^{-44} q N^2 T^4 \pi R^3. \quad (5)$$

Next, we consider the mean-free path of photons ( $l_{\text{photon}}$ ). The mean-free path of the photoionization ( $l_{p,i}$ ) is  $l_{p,i} = 1/\sigma_{bf} N_n$ , where  $\sigma_{bf}$  is the cross section of photoionization and  $N_n$  is the number density of highly excited atoms. In the present calculation,  $\sigma_{bf} = 10^{-20}$  (m<sup>2</sup>) and  $N_n = qN$  are assumed. It should be noted that the cross sections of photoionization listed in the literature [22] are usually those for the case where the initial state is the ground state, while it is a highly excited state in the present case. The mean-free path of photons by free-free transition (bremsstrahlung) ( $l_{f,f}$ ) is [17]  $l_{f,f} = (2.34 \times 10^{-2} T^{-1/2} q^2 N^2 \nu^{-3})^{-1}$ , where  $\nu$  is the frequency of the photon. The mean-free path of photons should be larger than the wavelength of the photons ( $\lambda_{\text{photon}}$ ) in the present case, because the emission of a photon is completed after it moves its wavelength. Thus, in the present simulation, the mean-free path of photons ( $l_{\text{photon}}$ ) is estimated by  $l_{\text{photon}} = \max[\lambda_{\text{photon}}, \min(l_{p,i}, l_{f,f})]$ . In the present study,  $\lambda_{\text{photon}} = hc/kT$  is assumed, where  $h$  is the Planck constant and  $c$  is the light velocity.

The escape rate of the emitted photons from the bubble ( $r_e$ ) is assumed to be  $r_e = [R^3 - (R - l_{\text{photon}})^3]/R^3$ , when  $l_{\text{photon}} \leq R$ . When  $R \leq l_{\text{photon}}$ , ( $r_e = 1$ ) is assumed. The intensity of the emitted light from the bubble ( $I$ ) is estimated by  $I = (r_r h \bar{v} + P_{Br,ion} + P_{Br,atom}) r_e$ , where  $h \bar{v}$  is the mean en-

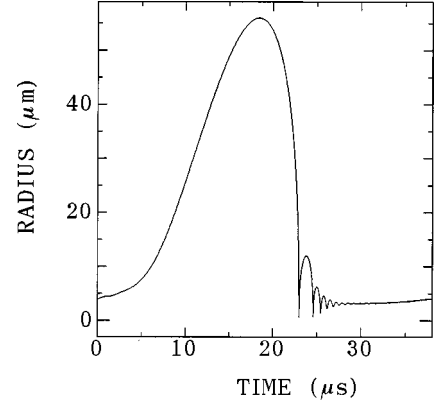


FIG. 1. Calculated radius-time curve for one acoustic cycle (38  $\mu$ s).

ergy of a photon emitted by radiative recombination. In the present calculation,  $h \bar{v} = \frac{3}{2} kT$  is assumed.

### III. RESULTS

The computer simulation is performed under a condition of SBSL [3]: a single bubble in 20 °C water driven by the acoustic wave whose frequency and amplitude are 26.4 kHz and 1.47 bar, respectively. An argon bubble is studied based on the Lohse's hypothesis [23] that a SBSL bubble in water containing air consists mainly of argon.

The ambient bubble radius is determined as 4  $\mu$ m to reproduce the maximum radius of 56  $\mu$ m [3]. The calculation starts from  $t=0$  and at first the bubble expands due to the negative acoustic pressure. It reaches the maximum radius of 56  $\mu$ m at  $t=18.4 \mu$ s as shown in Fig. 1. Then it begins to collapse rapidly to the minimum bubble radius of 0.6  $\mu$ m at  $t=22.9985 \mu$ s. The calculated results at around the minimum bubble radius for 2000 ps (0.002  $\mu$ s) are shown in Figs. 2(a)–2(f). In Fig. 2(a), the bubble radius is shown. In Fig. 2(b), the temperature inside the bubble is shown. It is seen that the temperature increases up to 20 000 K. In Fig. 2(c), the intensity of the emitted light from the bubble is shown; the line is the result of the present simulation and the dotted line is the result estimated by Stefan-Boltzmann's law of blackbody radiation [17]. It is seen that both the pulse width and the intensity calculated by the present model are smaller than those predicted by the blackbody formula. The pulse width is 80 ps, while that estimated by the blackbody formula is 170 ps. The maximum intensity is 3 mW, while that estimated by the blackbody formula is 40 mW. The light emission is mainly by radiative recombination of electrons and ions and electron-atom bremsstrahlung as shown in Fig. 2(d); the dash-dotted line is the intensity of the light emitted by radiative recombination, the dotted line is that emitted by electron-atom bremsstrahlung, and the dashed line is that emitted by electron-ion bremsstrahlung. It should be noted that the scale of the vertical axis of Fig. 2(d) is about an order of magnitude smaller than that of Fig. 2(c). The much shorter pulse width compared with that estimated by the blackbody formula is due to the fact that the light is emitted only when an appreciable amount of electrons exists inside the bubble. As seen in Fig. 2(e), the degree of ionization ( $q$ ) changes in a very short time due to the exponential depen-

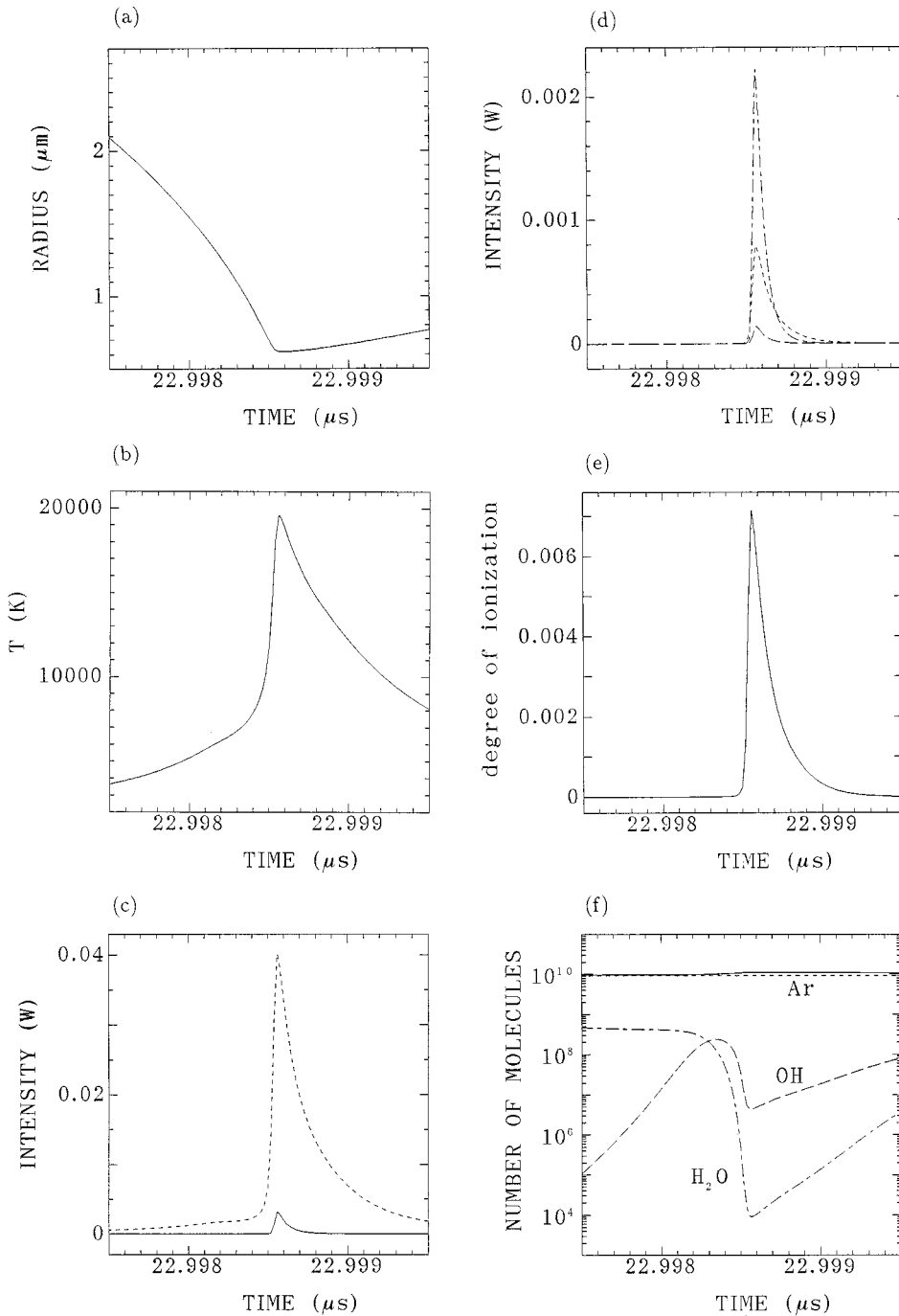


FIG. 2. Calculated results around the minimum bubble radius as functions of time for 2000 ps (0.002 μs). The time axes are the same throughout the figures. (a) The bubble radius ( $R$ ); (b) the temperature inside the bubble ( $T$ ); (c) the light intensity. The line is the intensity calculated by the present model and the dotted line is that estimated by the Stefan-Boltzmann law of blackbody radiation; (d) the intensity of the light emitted by radiative recombinations (dash-dotted line), that by electron-atom bremsstrahlung (dotted line), and that by electron-ion bremsstrahlung (dashed line); (e) the degree of ionization ( $q$ ); and (f) the number of molecules inside the bubble. The line is the total number of molecules, the dotted line is the number of argon molecules, the dash-dotted line is that of water vapor molecules, and the dashed line is that of OH molecules.

dence on temperature (Saha equation). The light emission starts and finishes as the degree of ionization increases and decreases, respectively. It means that the pulse width is nearly independent of wavelength, as experimentally observed [24,25], because the lights of any wavelength turn on and off by the same mechanism.

In Fig. 2(f), the number of molecules inside the bubble is shown; the line is the total number of molecules inside the bubble, the dotted line is the number of argon molecules, the dash-dotted line is that of water vapor molecules, and the dashed line is that of OH molecules. It is seen that almost all the vapor molecules are dissociated. The chemical reactions decrease the bubble temperature considerably as already pointed out in Ref. [8]. At the last 1500 ps of the collapse, the internal energy of the bubble increases by  $3.7$

$\times 10^{-9}$  (J), due both to the pV (pressure-volume change) work by the surrounding liquid [ $5.7 \times 10^{-9}$  (J)] and the change of the macroscopic kinetic energy of gases to heat at the end of the collapse [ $1.0 \times 10^{-9}$  (J)]. The reduction of the energy is mainly by thermal conduction [ $-1.9 \times 10^{-9}$  (J)] and the heat of chemical reactions [ $-1.1 \times 10^{-9}$  (J)].

The present formulation of bubble dynamics described in Ref. [8] is a rather crude one because it is assumed that temperature is spatially uniform inside a bubble except at the thermal boundary layer and pressure is spatially uniform inside a bubble. Nevertheless, the present model [8] has the advantage that the effect of chemical reactions is taken into account while in the first principles calculations of the hydrodynamic equations it is practically impossible because the rates of chemical reactions spatially vary in such a model.

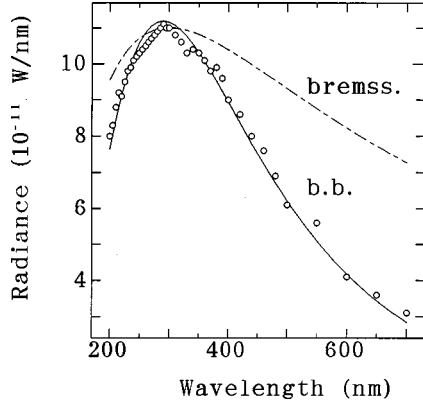


FIG. 3. Spectrum of SBSL from a bubble of the mixture of 2% Xe and 98%  $N_2$  in water. The open circles are the experimental data [14], the line is the calculated blackbody spectrum with the effective temperature of 10 000 K, and the dash-dotted line is that of thermal bremsstrahlung with the effective temperature of 32 000 K. It should be noted that the absolute values of the calculated spectra are arbitrarily determined just to see the shape of the spectra.

#### IV. SPECTRA OF SBSL

The following is the theoretical analysis of the spectra of SBSL experimentally observed by Hiller *et al.* [14,15].

The reported spectra of SBSL are all continuous and have no characteristic lines such as the OH line [14,15]. In Fig. 3, the spectrum of SBSL from a bubble of the mixture of 2% Xe and 98%  $N_2$  in water is shown by open circles [14]. The line is the calculated blackbody spectrum with the effective temperature of 10 000 K and the dash-dotted line is that of thermal bremsstrahlung with the effective temperature of 32 000 K. It should be noted that the calculated curves represent just the shape of the spectra, and the absolute values are arbitrarily determined.

The spectral radiance of the blackbody radiation is proportional to  $\lambda^{-5}[\exp(hc/kT\lambda)-1]^{-1}$ , where  $\lambda$  is the wavelength,  $h$  is the Planck constant,  $c$  is the light velocity,  $k$  is the Boltzmann constant, and  $T$  is the temperature [17]. The spectral radiance of thermal bremsstrahlung is proportional to  $\lambda^{-1.5} \exp(-hc/kT\lambda)$  [7].

From Fig. 3, it is seen that the experimentally observed spectrum [14] is fitted by the blackbody formula remarkably well, while it is not fitted by the formula of thermal bremsstrahlung. All the experimentally observed spectra described in Refs. [14,15] are well fitted by the blackbody formula, while they are not fitted by the formula of thermal bremsstrahlung. Thus, it is concluded that the bare thermal bremsstrahlung is excluded as the mechanism of SBSL, though it is regarded as the mechanism in some theoretical works [4,7].

From the above analysis, an important question arises: Why is the spectrum of SBSL fitted by the blackbody formula remarkably well, despite the fact that the result of the computer simulation indicates that SBSL is not the blackbody radiation [Fig. 2(c)]? The solution is Kirchhoff's law that the source function ( $S_\nu$ ) of thermally emitting material is equivalent to the Planck function [ $B_\nu(T)$ ], where  $S_\nu$  is defined as the ratio of the emission coefficient ( $j_\nu$ ) to the absorption coefficient ( $\alpha_\nu$ ) ( $S_\nu = j_\nu/\alpha_\nu$ );  $j_\nu$  is defined as the energy of the light of frequency  $\nu$  emitted per unit time per

unit frequency per unit solid angle and per unit volume,  $\alpha_\nu$  is defined as the loss of the intensity of light of frequency  $\nu$  per unit distance divided by the specific intensity ( $I_\nu$ ),  $I_\nu$  is defined as the energy of light of frequency  $\nu$  crossing unit area per unit time per unit solid angle and per unit frequency, and  $B_\nu(T) = 2h\nu^3 c^{-2} / [\exp(h\nu/kT) - 1]$ , which, in other words, is the blackbody formula [17]. The equation of the radiative transfer is given by [17]

$$\frac{dI_\nu}{ds} = -\alpha_\nu I_\nu + j_\nu = -\alpha_\nu I_\nu + \alpha_\nu B_\nu(T), \quad (6)$$

where  $s$  is a distance and Kirchhoff's law is used. The solution of Eq. (6) is

$$I_\nu(s) = [I_\nu(0) - B_\nu(T)]e^{-\alpha_\nu s} + B_\nu(T). \quad (7)$$

It is seen that the spectrum of the thermal radiation is the blackbody type [ $\propto B_\nu(T)$ ] from the beginning [in this case,  $I_\nu(0) = 0$ ]. After passing a distance much longer than  $1/\alpha_\nu$ , the radiation reaches the complete thermodynamic equilibrium, blackbody radiation [ $I_\nu = B_\nu(T)$ ]. The answer to the above question is that SBSL is not the blackbody radiation but the thermal radiation.

From the above discussion, it is also concluded that the effective blackbody temperature observed experimentally [3,14,15] is the real temperature inside the bubble. It supports the quasiadiabatic compression model because the effective blackbody temperature observed (10 000–20 000 K [3,14,15]) coincides with the bubble temperature predicted by the quasiadiabatic model (10 000–20 000 K [8,26]).

Next, the intensity of SBSL is considered. According to the calculated results in Sec. III, the mean-free path of photons is determined by the wavelength of the light. The wavelength of the visible light (0.2–0.8  $\mu\text{m}$ ) is comparable to the minimum bubble radius (0.6  $\mu\text{m}$ ). Thus, SBSL emission is nearly a volume emission; the intensity is nearly proportional to the bubble volume ( $\frac{4}{3}\pi R_{\min}^3$ , where  $R_{\min}$  is the minimum bubble radius). It should be noted that the blackbody radiation is a surface emission and the intensity is proportional to the emitting area [17]. Thus the intensity of SBSL ( $I_{\text{SBSL}}$ ) is estimated by

$$I_{\text{SBSL}} = \frac{4}{3}\pi R_{\min}^3 (rh\bar{\nu}\Delta t)f, \quad (8)$$

where  $r$  is the rate of the microscopic emission process per unit volume and unit time,  $h$  is the Planck constant,  $\bar{\nu}$  is the mean frequency of the emitted light,  $\Delta t$  is the pulse width of SBSL (duration of the light emission), and  $f$  is the frequency of the ultrasound (the number of SBSL flashes per unit time). It should be noted that for the blackbody radiation the intensity is determined by the emitting area, temperature, pulse width, and frequency of the ultrasound [ $I_{\text{b.b.}} = (\pi^2 k^4 / 60 c^2 \hbar^3) T^4 \times 4\pi R_{\min}^2 f \Delta t$ , where  $k$  is the Boltzmann constant and  $\hbar = h/2\pi$ ]. It is seen from Eq. (8) that SBSL intensity from noble gases strongly depends on the degree of



ionization of the gas ( $q$ ), because  $r$  is proportional to  $q^2$  [radiative recombination, Eq. (3)] or  $q$  [electron-atom bremsstrahlung, Eq. (5)].

## V. CONCLUSION

The mechanism of SBSL is investigated theoretically based on the quasiadiabatic compression model. It is concluded that SBSL is not the blackbody radiation but the ther-

mal radiation. The shape of the spectrum is determined by the bubble temperature and the intensity is determined by the rates of the microscopic processes of the light emission. For a noble-gas bubble, radiative recombination of electrons and ions and electron-atom bremsstrahlung are the dominant microscopic processes of the light emission. The pulse width is almost independent of wavelength for a noble-gas bubble because the light of any wavelength is emitted only when an appreciable amount of electrons exists inside the bubble.

- 
- [1] L. A. Crum, *Phys. Today* **47** (9), 22 (1994).
  - [2] D. F. Gaitan, Ph.D. thesis, University of Mississippi, 1990; D. F. Gaitan, L. A. Crum, C. C. Church, and R. A. Roy, *J. Acoust. Soc. Am.* **91**, 3166 (1992).
  - [3] B. P. Barber, R. A. Hiller, R. Löfstedt, S. J. Putterman, and K. R. Weninger, *Phys. Rep.* **281**, 65 (1997).
  - [4] C. C. Wu and P. H. Roberts, *Phys. Rev. Lett.* **70**, 3424 (1993).
  - [5] W. C. Moss, D. B. Clarke, J. W. White, and D. A. Young, *Phys. Fluids* **6**, 2979 (1994).
  - [6] L. Kondic, J. I. Gersten, and C. Yuan, *Phys. Rev. E* **52**, 4976 (1995).
  - [7] H. Kwak and J. H. Na, *Phys. Rev. Lett.* **77**, 4454 (1996).
  - [8] K. Yasui, *Phys. Rev. E* **56**, 6750 (1997).
  - [9] K. R. Weninger, H. Cho, R. A. Hiller, S. J. Putterman, and G. A. Williams, *Phys. Rev. E* **56**, 6745 (1997).
  - [10] V. Q. Vuong and A. J. Szeri, *Phys. Fluids* **8**, 2354 (1996).
  - [11] V. Q. Vuong, A. J. Szeri, and D. A. Young, *Phys. Fluids* **11**, 10 (1999).
  - [12] L. Yuan, H. Cheng, M. Chu, and P. Leung, *Phys. Rev. E* **57**, 4265 (1998).
  - [13] H. Cheng, M. Chu, P. Leung, and L. Yuan, *Phys. Rev. E* **58**, R2705 (1998).
  - [14] R. Hiller, K. Weninger, S. J. Putterman, and B. P. Barber, *Science* **266**, 248 (1994).
  - [15] R. Hiller, Ph.D. thesis, University of California, 1995.
  - [16] K. Yasui, *J. Acoust. Soc. Am.* **98**, 2772 (1995).
  - [17] G. B. Rybicki and A. P. Lightman, *Radiative Processes in Astrophysics* (Wiley Interscience, New York, 1979).
  - [18] A. von Engel, *Ionized Gases* (AIP, New York, 1994).
  - [19] S. C. Brown, *Basic Data of Plasma Physics* (AIP, New York, 1994).
  - [20] L. Frommhold, *Phys. Rev. E* **58**, 1899 (1998).
  - [21] R. L. Taylor and G. Caledonia, *J. Quant. Spectrosc. Radiat. Transf.* **9**, 657 (1969).
  - [22] H. S. W. Massey, *Electronic and Ionic Impact Phenomena* (Clarendon Press, Oxford, 1969), Vol. 2.
  - [23] D. Lohse, M. P. Brenner, T. F. Dupont, S. Hilgenfeldt, and B. Johnston, *Phys. Rev. Lett.* **78**, 1359 (1997).
  - [24] B. Gompf, R. Günther, G. Nick, R. Pecha, and W. Eisenmenger, *Phys. Rev. Lett.* **79**, 1405 (1997).
  - [25] R. Hiller, S. J. Putterman, and K. R. Weninger, *Phys. Rev. Lett.* **80**, 1090 (1998).
  - [26] K. Yasui, *Phys. Rev. E* **58**, 4560 (1998).